Supplementary Methods

For an overview of the performance of different read aligners and binding site detection algorithms on 10 simulated PAR-CLIP datasets, we calculated the precision, recall and accuracy for each. We considered all reads originating from simulated RBP-binding sites (with T–C conversions) as positives and those originating from other areas of the reference (simulated contaminations) as negatives. True positive and negative reads are those which are aligned correctly, whereas false positive and negative reads are those which are wrongly or not aligned (Table 1; Supplementary Table 3). We used BMix, PARalyzer and our hierarchical clustering to obtain the read clusters. Filtering of the clusters generated with the hierarchical clustering was performed as described in Section 2.2. A correctly reported binding site was considered a true positive, a falsely reported cluster (simulated contamination without elevated T–C conversions) as a false positive, an unreported binding site as a false negative and an unreported cluster (without T–C conversions) as a true negative (Supplementary Table 4). Unfortunately, BMix does not report false negative clusters (contaminations) and thus we were not able to calculate the recall nor the accuracy, but only the precision.

Execution commands

Quality and adapter trimming:

```
cutadapt -e 0.05 -q 28 -m 18 -b $adapter -f fastq -o $output $input
```

Alignment:

```
bwa aln -n $n $hg38_reference $trimmed_input > $output.sai ($n in {1, 2, 0.01, 0.02, 0.04})
bwa samse $hg38_reference $output.sai $trimmed_input > $output.sam
bowtie -S -v 1 --best -m $n --strata $hg38_reference -q $trimmed_input $output.sam ($n in {1,
        2})
bowtie2 -x $hg38_reference -U $trimmed_input -S $output.sam
parasuite map --refine -q $trimmed_input -r $hg38_reference -t $hg38_transcriptome -o
        $output --parasuite-mm $X ($X in {1, 2, 3, -1})
STAR --genomeDir $hg38_reference --readFilesIn $trimmed_input --outFileNamePrefix $output
subjunc -u -n -i $hg38_reference -r $trimmed_input -o $output.sam
tophat -o $output $hg38_reference $trimmed_input
```

```
MosaikBuild -q $trimmed_input -out $mosaik_input -st illumina -ga hg38
MosaikAligner -ia $hg38_reference -in $mosaik_input -out $output -mm 3 -annse ./mosaik-2.2.3/network_files/2.1.78.se.ann -annpe ./mosaik-2.2.3/network_files/2.1.78.pe.ann -m unique -bw 5
```

RBP binding site detection:

PARalyzer config file:

```
BANDWIDTH=3
CONVERSION=T>C
MINIMUM_READ_COUNT_PER_CLUSTER=5
MINIMUM_READ_COUNT_FOR_KDE=3
MINIMUM_CLUSTER_SIZE=14
MINIMUM_CONVERSION_LOCATIONS_FOR_CLUSTER=1
MINIMUM_CONVERSION_COUNT_FOR_CLUSTER=1
MINIMUM_READ_COUNT_FOR_CLUSTER_INCLUSION=5
MINIMUM_READ_LENGTH=13
MAXIMUM_NUMBER_OF_NON_CONVERSION_MISMATCHES=0
MINIMUM_READ_COUNT_PER_GROUP=5
EXTEND_BY_READ
```

BMix config file:

```
COV_MIN=5
REFINE_COV=1
CONFIDENCE_PER=0.95
SEPARATE_STRANDS=1
```

PARA-suite clustering:

```
parasuite clust $alignment.bam $hg38_reference $output $dbsnp_142 5
```

Annotation:

```
annotatePeaks.pl $clusters.peak hg38 -norevopp -strand "+" > $clusters.annotated
```

Supplementary Results

Simulation of uridylate-rich and homopolymeric PAR-CLIP reads

To measure the accuracy of the PARA-suite aligner for special types of data (uridylate-rich sequences, which are common in PAR-CLIP and homopolymeric sequences), we generated subsets of our simulated data that contained either >35% T (uridylate-rich sequences) or homopolymeric sequences with stretches of five or more bases of a particular nucleotide.

For the uridylate-rich PAR-CLIP reads, we observed an increase of 1.37% for PARA-suite alignments and an increase of 2.35% in the accuracy for BWA PSSM alignments compared to our basic simulated data (Supplementary Table 5). The accuracy for the PARA-suite decreased by 1.53% but the accuracy was unchanged for BWA PSSM when the PARA-suite was applied to the homopolymeric PAR-CLIP reads (Supplementary Table 5).

Application of the PARA-suite to HITS-CLIP data

Besides PAR-CLIP, other CLIP protocols are also used widely. Therefore, we chose a previously published Argonaute protein HITS-CLIP dataset generated from mouse brain samples (Chi, Zang et al. 2009) to assess the PARA-suite on a different type of CLIP data. To allow a comparison to previous results on the same dataset, we excluded all sequencing reads that were shorter than 25 bases after quality trimming using cutadapt. Next, we determined the error profile for the pooled replicates of the HITS-CLIP dataset using the respective PARA-suite tool to train its alignment pipeline. Here, we could already verify the high rate of deletions in contrast to insertions or single nucleotide substitutions compared to the mouse reference genome sequence GRCm38 (Chinwalla, Cook et al. 2002). Next, we applied the alignment pipeline to the pooled sequencing reads to align them against GRCm38 and against the transcript database of Ensembl genes Version 77 for the mouse genome assembly, and combined the results. Again, the transcriptomic mapping step revealed 79,658 additional aligned reads spanning exon–exon junctions out of 15,145,095 aligned reads in total (0.526 %). To achieve comparable results for RBP-bound transcribed regions in the mouse genome, we used PIPE-CLIP (Chen, Yun et al. 2014), which is a web-based program for cluster enrichment analysis of CLIP sequencing data. We compared our results with the number of cross-linked regions reported in the PIPE-CLIP publication analyzing the same dataset. The filtering criteria were the same as those in the PIPE-CLIP publication with an enriched cluster length of ≥25 bases and exclusion of duplicated sequencing reads by mapping position. After filtering the entire list of cross-linked regions for those that were supported by deletions in the cross-linked sites, we found 1450 significantly enriched regions by applying false discovery rate (FDR) ≤0.01 filtering. This number was substantially larger than what was found by the initial PIPE-CLIP analysis based on read alignments using Novoalign (http://www.novocraft.com) with 1232 cross-linked regions that were supported by deletions, an increase of 17.69% identified regions in total.

We also applied FDR ≤0.001 filtering to compare our results with the first in-depth analysis of the same data (Zhang and Darnell 2011), which used a cross-linking-induced mutation sites (CIMS) analysis. We identified 984 cross-linked regions showing a reliable deletion, whereas the CIMS analysis applied to the read alignments performed by Novoalign identified only 886 cross-linked regions (Zhang and Darnell 2011).

Supplementary Tables and Figures

Supplementary Table S1: Statistics of *FET* PAR-CLIP reads (Hoell, Larsson et al. 2011) before and after filtering for confident clusters.

Dataset	**Reads in clusters**	**Reads in confident clusters**	**% reads passing the filter**
EWSR1	1,375,517	700,936	50.96
FUS	1,249,406	923,904	73.95
TAF15	1,310,291	761,710	58.13

Supplementary Table S2: Average numbers for 10 simulated PAR-CLIP datasets.

Simulated reads	1,326,151
Mean read length	23
Clusters	85,691
T–C conversions	624,737
Sequencing errors	367,325
Indels	7324

Supplementary Table S3: Average performance of short read aligners on 10 simulated PAR-CLIP datasets sorted by accuracy. The runtime for BWA PARA was determined without error profile estimation, whereas the runtime for the entire PARA-suite pipeline includes error profile estimation, and alignment against genomic and transcriptomic reference sequences and both of these in combination. The results for "PARAsuite pipeline" refer to an execution where the parameter X was automatically evaluated (default). The results for "PARAsuite X1", "X2" and "X3" refer to executions with fixed values for X (i.e. X = 1, X = 2 and X = 3; see section "execution commands" for further information).

Aligner	**Accuracy (in %)**	**Variance**	**Recall (in %)**	**Precision (in %)**	**Mapped overall**	**Mapped correctly**	**CPU time (in s)**	**Real time (in s)**	**Memory (in GB)**
PARAsuite pipeline	73.14	1.37E-06	84.49	71.85	1,024,792	969,948	2287.3	396.8	6.27
PARAsuite X3 pipeline	72.61	1.26E-06	84.57	70.76	1,057,149	962,901	1365.9	307.7	6.21
PARAsuite X2 pipeline	71.63	1.31E-06	83.39	70.35	993,244	949,870	3786.6	539.2	6.33
PARAsuite	69.74	1.38E-06	82.16	68.24	975,672	924,802	1189.7	153.7	4.42
PARAsuite X3	68.57	1.46E-06	81.85	66.36	995,213	909,390	356.6	73.0	4.42
PARAsuite X2	68.26	1.33E-06	81.04	66.79	945,035	905,293	2405.1	265.1	4.42
BWA 002	68.17	1.38E-06	82.32	64.98	959,235	904,090	3621.9	359.2	4.42
BWA 004	68.17	1.37E-06	82.31	64.98	959,171	904,034	3981.5	390.7	4.42
BWA 2MM	68.17	1.37E-06	82.31	64.98	959,171	904,034	795.5	109.5	4.42
BWA 001	66.73	1.46E-06	80.61	64.26	958,919	884,964	797.2	109.5	4.42
Bowtie 2MM	63.38	1.10E-06	77.91	60.93	886,512	840,540	713.2	120.6	4.46
BWA PSSM	59.80	1.18E-06	74.04	58.72	818,895	793,007	232.4	25.4	2.26
TopHat	59.69	8.35E-07	76.10	55.35	844,902	791,549	592.9	282.9	-
BWA 1MM	59.29	8.68E-07	77.01	53.26	808,033	786,330	76.8	13.4	3.32
Bowtie2	56.22	1.11E-06	73.23	51.43	763,893	745,531	93.8	45.8	4.41
Bowtie 1mm	56.19	1.11E-06	73.20	51.42	763,631	745,227	1016.3	268.0	6.12
PARAsuite X1 pipeline	53.02	8.44E-07	68.55	51.20	716,838	703,161	54.0	10.8	2.26
PARAsuite X1	50.85	9.15E-07	66.52	49.08	685,788	674,399	75.0	43.7	4.41
STAR	50.74	9.10E-07	69.57	43.02	826,871	672,920	133.5	248.6	28.39
MOSAIK	44.88	2.18E-04	62.83	37.16	897,679	595,220	18,125.54	12,128.18	194.16
Subjunc	35.42	9.03E-07	50.61	26.09	597,400	469,751	24.3	64.2	6.65

Supplementary TableS 4: Binding sites detected by BMix, PARalyzer and the hierarchical clustering applied to read alignments of 10 simulated PAR-CLIP datasets. Recall and accuracy cannot be calculated for BMix because it does not provide a list of negative (discarded) clusters.

Aligner	True positives	True negatives	False positives	False negatives	Precision (in %)
BWA 2mm BMix	29,631	0	1456	0	95.32
BWA 2mm clustering	30,516	17,587	1795	5229	94.45
BWA 2mm paralyzer	29,255	12,184	5684	1575	83.73
BWA PSSM BMix	28,440	0	1470	0	95.09
BWA PSSM clustering	29,130	15,993	1837	2222	94.07
BWA PSSM paralyzer	28,396	11,172	5663	952	83.37
Bowtie 1mm BMix	26,824	0	969	0	96.51
Bowtie 1mm clustering	27,234	16,230	1137	3605	95.99
Bowtie 1mm paralyzer	27,464	11,252	5223	1299	84.02
Bowtie 2mm BMix	28,061	0	1375	0	95.33
Bowtie 2mm clustering	28,911	16,359	1691	4491	94.47
Bowtie 2mm paralyzer	27,979	11,218	5303	1280	84.07
Bowtie2 BMix	26,832	0	969	0	96.52
Bowtie2 clustering	27,231	16,239	1138	3611	95.99
Bowtie2 paralyzer	29,631	0	1456	0	84.03
PARA-suite BMix	31,918	0	1908	0	94.36
PARA-suite clustering	32,995	17,940	2394	4065	93.23
PARA-suite paralyzer	30,149	12,448	6329	2176	82.65

Supplementary Table S5: Alignment fractions of selected short read aligners applied to the PAR-CLIP results of the *FET* protein family. The PARA-suite aligner outperformed BWA 2MMs and BWA PSSM for all three datasets.

Dataset	Reads after trimming	PARA-suite aligner	PARA-suite aligner fraction	BWA PSSM	BWA PSSM fraction	BWA 2MMs	BWA 2MMs fraction
EWSR1	14,557,174	3,193,140	21.94%	2,350,935	16.15%	2,870,884	19.72%
FUS	10,981,718	3,571,035	32.70%	3,161,867	28.79%	3,083,820	28.08%
TAF15	10,611,969	2,457,585	23.16%	1,605,642	15.13%	2,326,287	21.92%

Supplementary Table S6: Accuracy of the PARA-suite and BWA PSSM on uridylate-rich and homopolymeric simulated PAR-CLIP data.

Aligner	**Accuracy**	
	Uridylate-rich	**Homopolymers**
PARA-suite	71.11	68.21
BWA PSSM	62.15	59.80

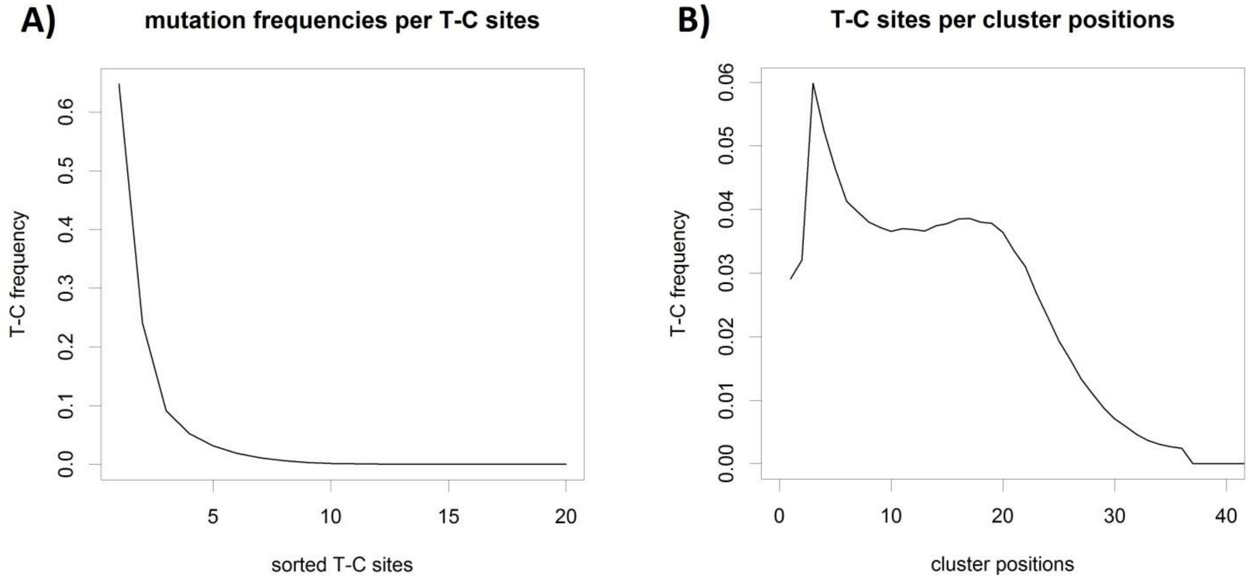

Supplementary Figure S1: (A) T–C conversion frequencies (α) in real PAR-CLIP data (summarized over all *FET* PAR-CLIPs (Hoell, Larsson et al. 2011)) and sorted by T–C sites within highly confident clusters. (B) Probabilities (β) for the preferred read positions of T–C conversion sites within confident clusters. This graph shows a peak at the beginning of the clusters where the majority of T–C conversions occurred.

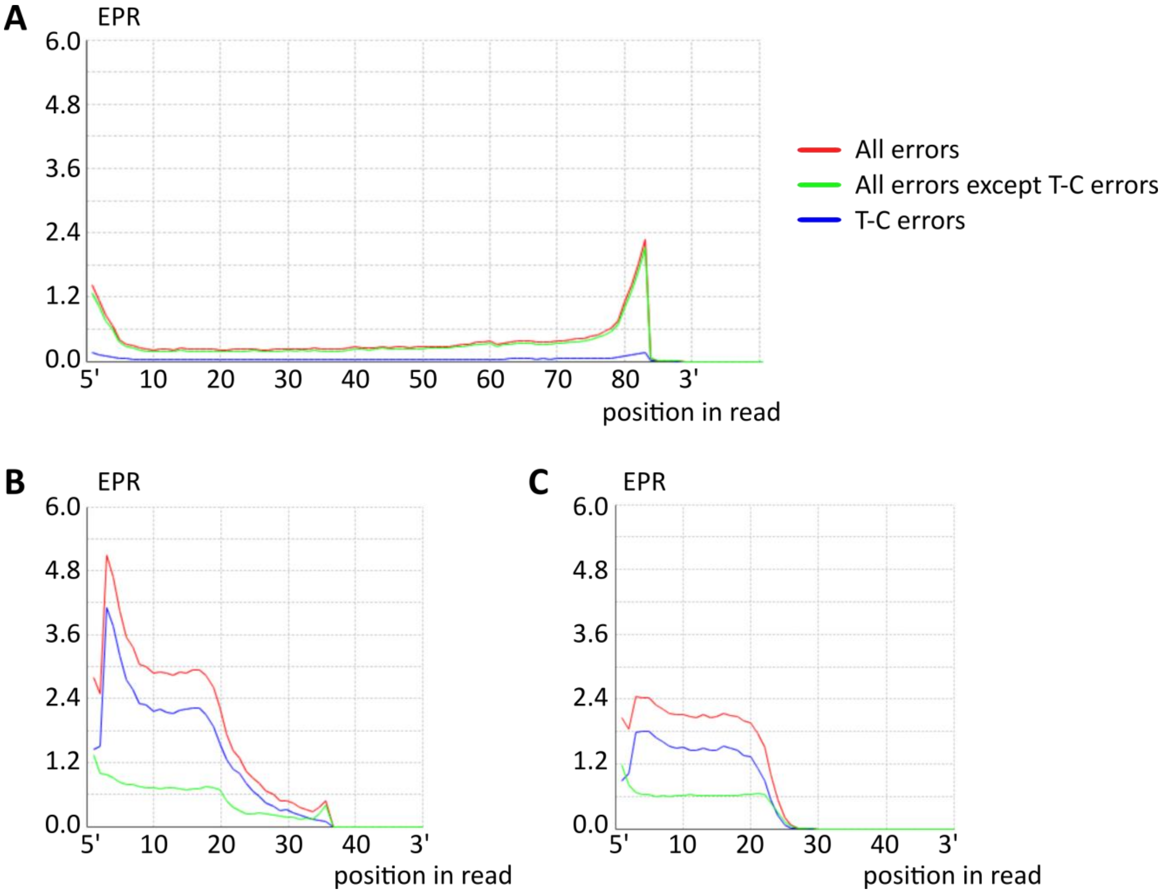

Supplementary Figure S2: Error profiles for (A) human reference RNA-Seq, (B) *FUS* PAR-CLIP and (C) simulated PAR-CLIP data (averaged over 10 simulated datasets) showing position-wise errors per reads × 100 (EPR). The RNA-Seq profile in (A) has higher sequencing error rates in the outermost bases and a very low average in the mid-range of the reads. The two PAR-CLIP error-profiles in (B) and (C) show a high increase in T–C errors between the read sequences and the reference sequence.

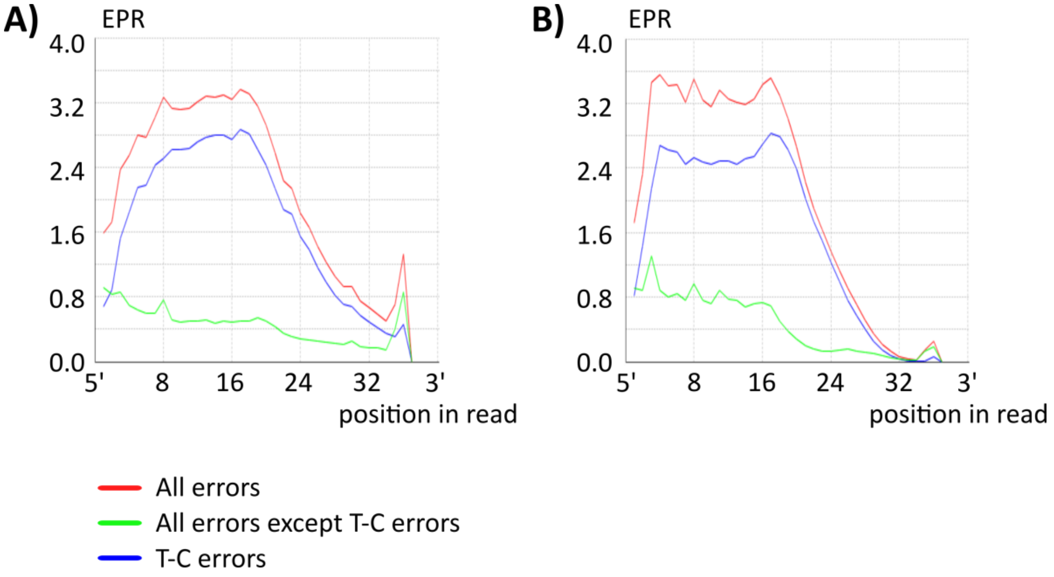

Supplementary Figure S3: Error profiles for (A) *HuR* (Mukherjee, Corcoran et al. 2011) and (B) *MOV10* (Sievers, Schlumpf et al. 2012). Both error profiles lack a peak in the error rate for the first bases but show nearly the same average T–C conversion frequencies as the *FET* PAR-CLIP dataset with 1.684 errors per reads × 100 (EPR) for *HuR* and 1.561 EPR for *MOV10* as compared to 1.477 EPR for, say, *FUS*.

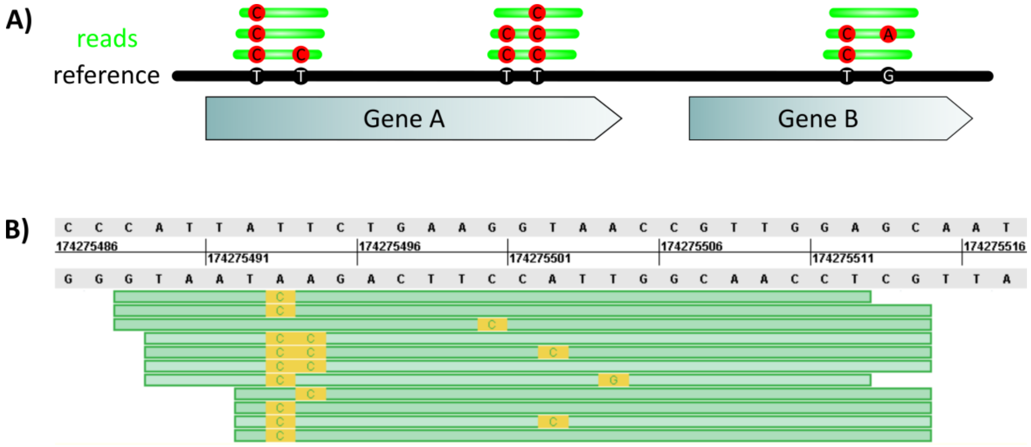
A)
reads
reference
C
C
C
C
T
T
C
C
C
C
C
T
T
C
A
C
T
G
Gene A
Gene B
B)
C C C A T T A T T C T G A A G G T A A C C G T T G G A G C A A T
174275486
174275491
174275496
174275501
174275506
174275511
174275516
G G G T A A T A A G A C T T C C A T T G G C A A C C T C G T T A
C
G

Supplementary Figure S4: (A) Schematic view of PAR-CLIP reads aligned against a reference sequence. All reads are stacked into three clusters covering only small parts of the respective genes. Furthermore, T–C conversion sites with high and low mutation frequencies as well as a G–A sequencing errors are shown. (B) Modified representation of a cluster of simulated PAR-CLIP sequencing reads, produced by GenomeView version 2350 (http://genomeview.org/). The cluster shows three T–C conversion sites, one of which has a very high amount of T–C conversions, and A–G and G–C sequencing errors.

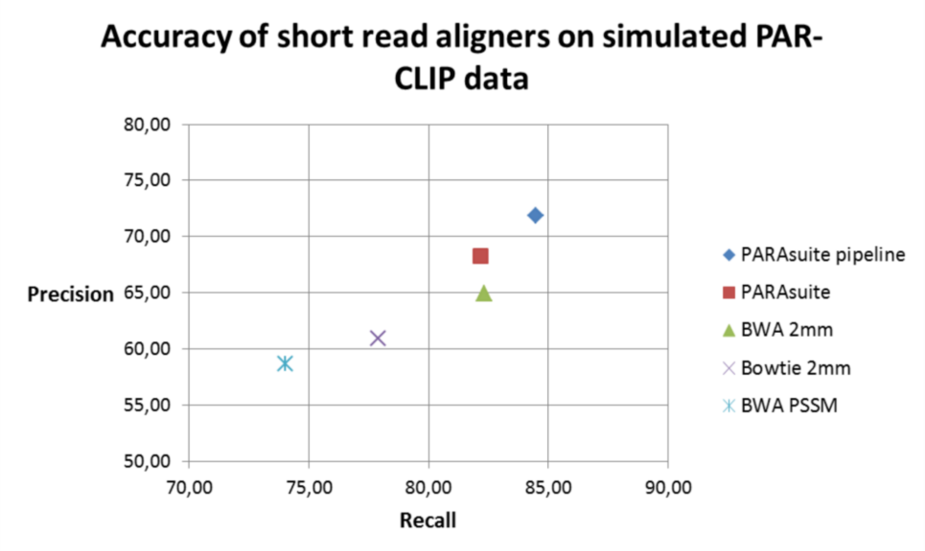

Supplementary Figure S5: Average accuracy of short read aligners on 10 simulated PAR-CLIP datasets. Bowtie and BWA were run allowing for two mismatches (Bowtie 2MMs and BWA 2MMs). The PARA-suite, including the transcriptome alignment (called the PARA-suite pipeline), outperformed all other aligners in recall and precision. The performance values obtained for additional aligners are listed in Supplementary Table 2.

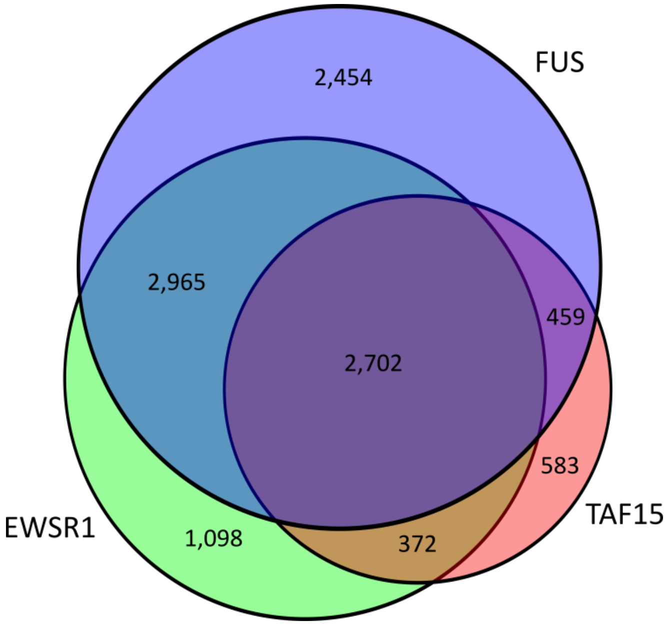

Supplementary Figure S6: Overlaps of genes targeted by the *FET* family identified by the cross-linked regions after cluster filtering. *P*-values for the Pairwise enrichments are as follows using Fisher's exact test: EWSR1–FUS enrichment = 2.1 (p-value < 0.000); FUS–TAF15 enrichment = 2.0 (p-value < 0.000); EWSR1–TAF15 enrichment = 2.4 (p-value < 0.000). The largest fraction of 2702 distinct genes is covered by all three datasets, which correlates with the results of the initial study.

Supplementary References

Chen, B., Yun, J., Kim, M. S., Mendell, J. T. and Xie, Y. (2014). PIPE-CLIP: a comprehensive online tool for CLIP-seq data analysis. *Genome Biol.* **15**: R18.

Chi, S. W., Zang, J. B., Mele, A. and Darnell, R. B. (2009). Argonaute HITS-CLIP decodes microRNA–mRNA interaction maps. *Nature* **460**(7254): 479-486.

Chinwalla, A. T., Cook, L. L., Delehaunty, K. D., Fewell, G. A., Fulton, L. A., Fulton, R. S., Graves, T. A., Hillier, L. W., Mardis, E. R. and McPherson, J. D. (2002). Initial sequencing and comparative analysis of the mouse genome. *Nature* **420**(6915): 520-562.

Hoell, J. I., Larsson, E., Runge, S., Nusbaum, J. D., Duggimpudi, S., Farazi, T. A., Hafner, M., Borkhardt, A., Sander, C. and Tuschl, T. (2011). RNA targets of wild-type and mutant FET family proteins. *Nat. Struct. Mol. Biol.* **18**(12): 1428-1431.

Mukherjee, N., Corcoran, D. L., Nusbaum, J. D., Reid, D. W., Georgiev, S., Hafner, M., Ascano, M., Tuschl, T., Ohler, U. and Keene, J. D. (2011). Integrative regulatory mapping indicates that the RNA-binding protein HuR couples pre-mRNA processing and mRNA stability. *Mol. Cell* **43**(3): 327-339.

Sievers, C., Schlumpf, T., Sawarkar, R., Comoglio, F. and Paro, R. (2012). Mixture models and wavelet transforms reveal high confidence RNA-protein interaction sites in MOV10 PAR-CLIP data. *Nucleic Acids Res.* **40**(20): e160.

Zhang, C. and Darnell, R. B. (2011). Mapping in vivo protein-RNA interactions at single-nucleotide resolution from HITS-CLIP data. *Nat. Biotechnol.* **29**(7): 607-614.